Heliyon 9 (2023) e18280

Contents lists available at ScienceDirect

Heliyon

journal homepage: www.cell.com/heliyon

Diversity, astaxanthin production, and genomic analysis of *Rhodotorula paludigena* SP9-15

Sukanya Phuengjayaem [a,b], Engkarat Kingkaew [c], Patcharaporn Hoondee [d], Pornchai Rojsitthisak [e], Boonchoo Sritularak [f], Worathat Thitikornpong [e], Somphob Thompho [g], Natapol Pornputtapong [b], Somboon Tanasupawat [b,*]

[a] *Department of Microbiology, Faculty of Science, King Mongkut's University of Technology Thonburi, Bangkok 10140, Thailand*
[b] *Department of Biochemistry and Microbiology, Faculty of Pharmaceutical Sciences, Chulalongkorn University, Bangkok 10330, Thailand*
[c] *Department of Biology, School of Science, King Mongkut's Institute of Technology Ladkrabang, Bangkok 10520, Thailand*
[d] *Division of Biology, Faculty of Science and Technology, Rajamangala University of Technology Krungthep, Bangkok 10120, Thailand*
[e] *Department of Food and Pharmaceutical Chemistry, Faculty of Pharmaceutical Sciences, Chulalongkorn University, Bangkok 10330, Thailand*
[f] *Department of Pharmacognosy and Pharmaceutical Botany, Faculty of Pharmaceutical Sciences, Chulalongkorn University, Bangkok 10330, Thailand*
[g] *Pharmaceutical Research Instrument Center, Faculty of Pharmaceutical Sciences, Chulalongkorn University, Bangkok 10330, Thailand*

ARTICLE INFO

Keywords:
Astaxanthin
Biosynthetic pathway
Genome
Putative gene
Rhodotorula paludigena
Yeast

ABSTRACT

Astaxanthin is a carotenoid known for its powerful antioxidant properties. This study focused on isolating yeast strains capable of producing astaxanthin from flower and fruit samples collected in Thailand. Out of 115 isolates, 11 strains were identified that produced astaxanthin. Molecular identification techniques revealed that these isolates belonged to two species: *Rhodotorula paludigena* (5 isolates) and *Rhodosporidiobolus ruineniae* (6 isolates). Whole-genome analysis of one representative strain, *R. paludigena* SP9-15, identified putative candidate astaxanthin synthesis-associated genes, such as *CrtE, CrtYB, CrtI, CrtS, CrtR, CrtW, CrtO,* and *CrtZ*. High-performance liquid chromatography (HPLC) and liquid chromatography-mass spectrometry (LC-MS) confirmed astaxanthin production. Further optimization of astaxanthin production was carried out by investigating the effects of various factors on the growth rate and astaxanthin production. The optimal conditions were 40 g/L glucose as a carbon source, pH 7.5, and cultivation at 25 °C with 200 rpm for 3 days. Under these conditions, *R. paludigena* SP9-15 synthesized biomass of 11.771 ± 0.003 g/L, resulting in astaxanthin with a content of 0.558 ± 0.018 mg/g DCW (dry cell weight), an astaxanthin yield of 6.565 ± 0.238 mg/L, and astaxanthin productivity of 2.188 ± 0.069 g/L/day. These findings provide insights into astaxanthin production using red yeast strains from Thailand and highlight the potential of *R. paludigena* SP9-15 for further application.

1. Introduction

Astaxanthin is a natural red pigment with powerful antioxidant properties. It has diverse applications in aquaculture, cosmetics, pharmaceuticals, food, feed, and medicine [1]. This vibrant compound offers a range of health benefits, including reducing inflammation, combating free radicals, exhibiting anticancer properties, and providing photoprotection. It also has positive effects on the

* Corresponding author.
E-mail address: Somboon.T@chula.ac.th (S. Tanasupawat).

https://doi.org/10.1016/j.heliyon.2023.e18280
Received 17 April 2023; Received in revised form 7 July 2023; Accepted 13 July 2023
Available online 16 July 2023

eyes, heart, skin, liver function, and immune system [2]. Additionally, astaxanthin is a natural pigment that can be obtained from plants, microalgae, and yeasts. *Haematococcus pluvialis* and certain bacteria are commonly used as sources. However, there are challenges associated with cultivating and extracting astaxanthin from *H. pluvialis*. Cultivating *H. pluvialis* in open freshwater ponds is time-consuming and resource-intensive [3]. The strict light and stress conditions required for astaxanthin production add to the challenges and costs [4]. Nevertheless, researchers are working towards optimizing production and finding sustainable extraction methods [5].

Alternatively, astaxanthin can be produced by various species of red yeasts, such as *Rhodotorula* [6–8], *Rhodosporidium* [9–11], *Sporidiobolus, Sporobolomyces, Cystofilobasidium*, *Kockovaella*, and *Xanthophyllomyces dendrorhous* (formerly *Phaffia rhodozyma*), which are known as producers of carotenoid pigments [4,5]. These yeasts have the ability to produce various pigments, including beta-carotene, gamma-carotene, torulene, torularhodin, and astaxanthin [12]. However, several factors can limit astaxanthin biosynthesis, including the availability of precursor molecules and the efficiency of the biosynthetic pathways [13]. Furthermore, environmental conditions, such as pH, temperature, and nutrient availability, can significantly impact astaxanthin production in microorganisms [14]. Additionally, astaxanthin yield, productivity, and the cultivation conditions employed can vary significantly depending on the microbial strain used [15]. Therefore, the astaxanthin biosynthetic pathway and cultivation conditions are essential for maximizing astaxanthin production.

This study aimed to investigate the diversity of astaxanthin-producing yeasts found in flowers and fruits. This research identified *Rhodotorula paludigena* SP9-15 as a novel microbial source for natural astaxanthin production. We evaluated the effects of various carbon, nitrogen, and physicochemical parameters on astaxanthin production and used statistical analysis to optimize the medium compositions in order to maximize the concentration of astaxanthin. Additionally, the genome and genes of *Rhodotorula paludigena* SP9-15 are of particular interest due to their potential for astaxanthin biosynthesis.

2. Materials and methods

2.1. Screening and isolation of red yeast for astaxanthin biosynthesis

The flower and fruit samples were collected from various provinces in Thailand, including two samples from Bangkok, eight samples from Suphan Buri, seven samples from Prachin Buri, one from Chiang Mai, and one from Chiang Rai. One gram of each sample was enriched in 15 mL of Yeast extract-Malt extract (YM) medium supplemented with chloramphenicol (100 μg/mL) to inhibit bacterial contamination. The composition of the YM medium was peptone (5.0 g/L), malt extract (3.0 g/L), yeast extract (3.0 g/L), and glucose (10.0 g/L), with a pH adjusted to 5.5 before cultivation. The samples were incubated at 25 °C for 72 h without shaking. Subsequently, the enriched samples were transferred onto YM agar plates and cultivated under the same conditions. The different colonies were picked and re-streaked to purify the isolates. Then, the purified isolates were cryopreserved in 20% glycerol and stored in a freezer, while long-term preservation was achieved through lyophilization. All isolates that exhibited red colonies were subjected to qualitative astaxanthin analysis using the thin-layer chromatography technique (TLC). The method was slightly modified from Ushakumari and Ramanujan [16]. Initially, 0.01 g of lyophilized cells (Lyophilization Systems, Inc., USA) with a dry cell weight (DCW) measurement were suspended in 1 mL of acetone and homogenized using a pestle motor for 3 min at room temperature. Subsequently, the resulting mixture was centrifuged at a speed of 6000×*g* for 10 min.

Twenty microliters of the extracted sample were precisely applied onto aluminum TLC silica gel 60 F254 plates (Merck, Germany). The plates were developed using a mobile phase, a 1:3 (v/v) mixture of acetone and hexane. After development, the presence of colored bands became instantly noticeable, and they were subsequently compared to the standard astaxanthin band (Dayang Chem, China) through observation under visible light. Finally, the R_f value was determined by the material's movement across the TLC sheet.

2.2. Identification and characterization of selected strains

2.2.1. Phenotypic characteristics

The colony appearances, including size, color, form, elevation, margin, and transparency, were observed on YM agar after cultivation at 25 °C for 48 h. Yeast cell morphology was examined under light microscopy. The positive isolates were analyzed to assess their morphological and biochemical characteristics, which were then compared to the characteristics described for type strains [17]. In addition, the carbon assimilation tests were carried out utilizing the ID 32C kit (BioMerieux, France) in accordance with the guidelines provided by the manufacturer.

2.2.2. Genotypic characteristics and identification

To amplify the 26S rRNA gene (LSU D1/D2 domain) using PCR, the NL1 (5′-GCATATCAATAAGCGGAGGAAAAG-3′) and NL4 (5′-GGTCCGTGTTTCAAGACGG-3′) were utilized as primers [18]. The PCR reaction mixture had a volume of 50 μL, which contained 5.0 μL of DNA template, 5.0 μL of 10X PCR Buffer, 4.0 μL of 2.5 mM dNTP, 1.5 μL of forward and reverse primer (10 pmol/μL each), 0.5 μL of Taq DNA polymerase, 4.0 μL of 25 mM $MgCl_2$, and 28.5 μL of ultrapure water. The thermocycling conditions consisted of an initial denaturation phase at 94 °C for 5 min, followed by 30 cycles of denaturation at 94 °C for 1 min, annealing at 52 °C for 1 min and 30 s, extension at 72 °C for 2 min and 30 s, and culminated with a final extension step at 72 °C for 10 min. After amplification, the PCR product was purified using the Gel/PCR DNA fragment extraction kit (Geneaid Biotech Ltd., Taiwan). The purified PCR products were sequenced in both directions using the Sanger sequencing technique (Celemics, Inc., Republic of Korea) and the resulting sequences were compared to the NCBI database through a blasting process. The phylogenetic tree of the 26S rRNA gene sequencing was

constructed by the maximum-likelihood (ML) [19] methods with bootstrap analysis based on 1000 replications using MEGA X [20].

2.3. Genome analysis and functional annotation

The genomic DNA of the potential astaxanthin strain, *R. paludigena* SP9-15, was extracted by collecting the yeast cells after 48 h of cultivation in YM broth at 25 °C. One milliliter of yeast cell culture was harvested by centrifugation at 6000×*g* at 4 °C for 10 min then the suspended samples were mixed with 200 μL of lysis buffer (containing 100 mM Tris, pH 8.0, 30 mM EDTA, pH 8.0, and 0.5% SDS). The suspension was then boiled in a water bath for 15 min. After cooling on ice for 1 h, 200 μL of 2.5 M potassium acetate (pH 7.5) was added, mixed well, and incubated suddenly on ice for 1 h. The supernatant was centrifuged at 12,000×*g* for 5 min at 4 °C and extracted twice with 1 volume of $CHCl_3$-isoamyl alcohol (24:1, v/v).

After centrifugation at 10,000×*g* for 5 min, the supernatant was mixed with an equal volume of cold isopropanol and centrifuged again at 10,000×*g* for 16 min at 4 °C.

The DNA pellet was sequentially washed with 70% and 90% ethanol followed by centrifugation at 10,000×*g*, 4 °C for 16 min. The DNA pellet was dried at 37 °C then dissolved in 30 μL of sterile ultrapure water and stored at −20 °C until further use.

The genome of *Rhodotorula paludigena* SP9-15 was sequenced using Illumina HiSeq Xten/Novaseq/MGI2000 platforms. The resulting reads underwent quality control and assembly using Velvet software. The resulting reads were quality-controlled and assembled using Velvet software, with gap-filling carried out using SSPACE and GapFiller [21–25]. Identification of coding genes in the genome was accomplished using the Augustus gene-finding software (version 3.3) [26]. Meanwhile, the detection of transfer RNAs (tRNAs) was performed using tRNAscan-SE with the default parameters, while the identification of rRNA was accomplished using Barrnap. The RNA families database (rfam) was used to identify other RNAs [27]. The ANI value between strain SP9-15 and closely related species was determined using FASTANI (version 1.3) [28]. The Prokka server was utilized to generate the circular genomic map and Venn diagram [29] and OrthoVenn2 web-based tool [30]. The coding genes were subjected to annotation using the National Center for Biotechnology Information (NCBI), while their functions were determined through the utilization of the Kyoto Encyclopedia of Genes and Genomes (KEGG) [31] and KOfamKOALA tools [32]. The identification of carbohydrate-active enzymes was carried out utilizing the dbCAN meta server (https://bcb.unl.edu/dbCAN2/blast.php) with HMMER: biosequence analysis employing profile hidden Markov models (version 3.3.2), and the CAZy database (http://www.cazy.org/) was used for family classification of the data generated by dbCAN [33,34].

The draft genome of the strain has been deposited at DDBJ/EMBL/GenBank under the accession number JAQJJA000000000.

2.4. Qualitative astaxanthin analysis

2.4.1. High-performance liquid chromatography (HPLC)

To extract astaxanthin from *R. paludigena* SP9-15 cells, the lyophilized cells (0.05 g DCW) were suspended in 5 mL of DMSO. After mixing the solution, we sonicated it at 37 kHz (Elmasonic E60H, Elma Schmidbauer GmbH, Singen, Germany) and 55 °C for 5 min to further break down the cells and release the astaxanthin. The solution was then centrifuged at 6000×*g* and 25 °C for 10 min to eliminate remaining debris, and the resulting supernatant was filtered through a 0.22-μm membrane filter. Astaxanthin identification was performed using HPLC with minor adjustments [35]. For this purpose, a UHPLC Nexera X2 system (Shimadzu, Japan) was utilized, comprising an LC-30AD binary pump, a SIL-30AC autosampler, a CTO-20AC Column oven, and an SPD-M30A detector.

A Lab Solutions chromatography workstation was installed on the computer-controlled system for data analysis. The chromatographic column used to separate astaxanthin was a GL Science InertSustain C18 column (4.6 mm × 150 mm, 5 μm). The HPLC system used a flow rate of 0.5 mL/min during the first 3 min of analysis and then increased to 1.0 mL/min for the remainder of the run (03.01–20.00 min). The astaxanthin was detected at a wavelength of 480 nm, and the column was maintained at a constant temperature of 30 °C. The sample injection volume was 5 μL, with mobile phase A containing a mixture of methanol, acetonitrile, ethyl acetate, and formic acid (75.9:12:12:0.1, v/v), while mobile phase B was methanol.

2.4.2. Liquid chromatography-mass spectrometry (LC-MS)

Astaxanthin was identified using LC-MS with slight modifications from a previously described method [35]. The mass spectrum of pigment was obtained using a UHPLC-Nexera series, which was equipped with a triple quadrupole mass spectrometer (LCMS-8060NX, Shimadzu, Japan).

The sample was separated using an InertSustain C18 column (150 mm × 4.6 mm i.d., 5 μm, GL Sciences, Japan) and eluted with a mobile phase consisting of methanol, acetonitrile, and ethyl acetate (76:12:12, v/v) for mobile phase A and methanol for mobile phase B. A sample of 10 μL was injected into the column, which was maintained at a constant temperature of 30 °C. The flow rate was adjusted to 1.0 mL/min throughout the analysis.

The analysis of astaxanthin was detected using a triple quadrupole mass spectrometer equipped with electrospray ionization (ESI) in negative mode. The optimization conditions for the sensitivity of the instrument were as follows: N_2 nebulizing gas flowing at a rate of 3 L/min, heating gas at 15 L/min, and drying gas at 6 L/min, while the interface temperature, DL temperature, and heat block temperature were set at 350 °C, 250 °C, and 350 °C, respectively.

The optimization of the MS/MS parameters for astaxanthin detection was conducted in multiple reaction monitoring (MRM) modes, utilizing a precursor ion of 595.38 (M-H)-and three product ions were generated at 513.20, 430.75, and 348.90, each with collision energy (CE) values of 25.0, 12.0, and 48.0, respectively. The samples were subjected to analysis using the negative scan mode of MS, and the mass-to-charge ratio (m/z) was recorded in the range of 100 to 2000 Da.

2.5. Astaxanthin production from the selected strain

2.5.1. Yeast and inoculum preparation

The inoculum for strain SP9-15 was prepared by transferring a loopful of the yeast culture grown on active YM agar to 50 mL of YM broth in 250 mL Erlenmeyer flasks, followed by incubation at 25 °C with shaking at 200 rpm for 48 h. The cells were collected by centrifugation at 6000×*g* for 10 min at 4 °C, followed by two washes and then resuspended in a 0.85% (w/v) NaCl solution. In preparation for the inoculum starter, the yeast suspension was adjusted to obtain an initial cell suspension containing an OD_{660} of 1.00 ± 0.1 for investigating the optimization of astaxanthin production.

2.5.2. Astaxanthin production

The astaxanthin production experiments followed a one-factor-at-a-time (OFAT) approach in triplicate. To enhance reliability, all experiments were conducted in triplicate, instilling confidence in the study's findings. The production medium, meticulously formulated based on the YM medium, acted as a strategic foundation for astaxanthin synthesis. The production medium, based on the YM medium, consisted of glucose, yeast extract, malt extract, and peptone. *R. paludigena* SP9-15 was cultured in 250 mL Erlenmeyer flasks at 25 °C and 200 rpm for 72 h. Different carbon sources (sucrose, fructose, maltose) were tested at a concentration of 10 g/L. The nitrogen source and pH of the production medium were kept consistent with the aforementioned conditions. Subsequently, the selected carbon source was further tested at varying concentrations ranging from 10 g/L to 50 g/L. The supplementation of inorganic nitrogen sources (potassium nitrate, ammonium sulfate, urea) were evaluated at equivalent amounts. Different temperatures (15 °C to 35 °C) and pH values (4.5–8.5) were also studied. The conditions yielding the highest astaxanthin yield were chosen. Cultivation periods ranging from 1 to 7 days were tested using the optimal conditions. Samples were collected at 1, 3, 5, and 7 days to assess astaxanthin production.

2.5.3. Cell recovery

The cells were collected by centrifugation at 6000×*g* at 4 °C for 10 min, washed twice with deionized water, and centrifuged again. The dry cell weight (DCW) of the lyophilized cells was then measured for further astaxanthin analysis.

2.5.4. Astaxanthin extraction

The astaxanthin extraction was carried out with slight modifications, as previously reported [36]. Briefly, 0.05 g of lyophilized cells was suspended in 5 mL of DMSO (Sigma-Aldrich, USA), sonicated at 37 kHz and 50 °C for 30 min (Elmasonic, E60H model, Germany). The resulting cell extract was then centrifuged at 6000×*g* and 4 °C for 5 min, and the extraction process was repeated until the supernatant turned colorless. The astaxanthin content in the supernatant was then quantitatively analyzed using a spectrophotometer.

2.5.5. Quantification analysis of astaxanthin production using spectrophotometry

The astaxanthin concentration was measured using a spectrophotometer (Hitachi U2900, Japan) at 530 nm, with pure DMSO serving as reference [36,37]. A standard curve was generated using astaxanthin concentrations of 0, 0.25, 0.5, 1, 2, 4, 6, and 8 μg/mL in DMSO, and the concentration of astaxanthin was calculated using the linear equation of the astaxanthin standard calibration curve (R^2 = 0.990). The results were reported as the average and standard deviation of triplicate experiments.

2.5.6. Statistical analysis

The ability of astaxanthin production from positive isolates and optimization of astaxanthin production from the selected isolates were evaluated in triplicate. The results are presented as the mean ± standard deviation (SD). Data analysis was conducted using SPSS statistical software for Windows, version 22. A one-way ANOVA was employed to compare individual factors, while Tukey's multiple range test was used for pairwise comparisons with a significance level of $\alpha = 0.05$.

3. Results and discussion

3.1. Screening and isolation of red yeast for astaxanthin biosynthesis

The flower and fruit samples were collected from various provinces in Thailand, as detailed in Table 1. A total of 115 isolates were obtained, out of which 19 isolates exhibited orange to red colonies, while 11 isolates showed a positive preliminary screening result for astaxanthin on TLC (Fig. 4a and 4b). It is noteworthy that all extracts showed an astaxanthin band with an R_f value of 0.28, similar to the astaxanthin standard. Consequently, the 11 isolates demonstrating astaxanthin production were chosen for further characterization in future experiments.

3.2. Identification and characterization of selected strains

The positive astaxanthin yeast strains exhibited circular, convex colonies with an entire margin and an opaque appearance. Under light microscopic examination, the cells were observed to have an oval shape. A slight variation in colony color was noted, with strains SP3-1, SP3-2, and SP3-5 displaying an old rose colony, while strains SP3-3/1, SP3-3/4, SP8-8/3, SP9-10, SP9-12/2, SP9-14, and SP9-15 exhibited a pink colony. The SP8-7/2 strain was the only one with an orange colony.

The distinctive carbon assimilation abilities of the isolates are presented in Table 2. All astaxanthin-producing isolates

Table 1
The information of samples, sampling locations, and enumeration of pigmented yeasts.

Sample no.	Source (Common, Scientific name)	Location	Number of isolates	No. of red pigmented yeast	No. Astaxanthin producing strains
Flower					
CU1	Bastard teak (*Butea monosperma*)	Bangkok	4	0	0
CU2	Bastard teak (*Butea monosperma*)	Bangkok	5	0	0
SP3	Red Cat's Tail (*Acalypha hispida* Burm.f.)	Suphan Buri	10	8	5
SP4	Wild Cockcomb (*Celosia argentea* L. var. *cristata* (L.) Kuntze)	Suphan Buri	7	0	0
SP5	Impala Lily (*Adenium obesum*)	Suphan Buri	7	2	0
SP7	Weeping Lantana (*Lantana camara* L.)	Suphan Buri	3	0	0
SP8	Red West Indian Jasmine (*Ixora coccinea* L.)	Suphan Buri	15	2	2
SP9	Zinnia (*Zinnia violacea* Cav.)	Suphan Buri	27	5	5
SP10	*Wodyetia bifurcata* A.K. Irvine	Suphan Buri	3	0	0
SP11	Variegata (*Asystasia gangetica* (L.) T. Anderson)	Suphanburi	5	0	0
PC1	Pink West Indian Jasmine (*Ixora coccinea* L.)	Prachin Buri	4	0	0
PC2	Yellow West Indian Jasmine (*Ixora coccinea* L.)	Prachin Buri	4	0	0
PC4	Ashoka (*Saraca asoca*)	Prachin Buri	2	0	0
PC5	Canna lily (*Canna indica* L.)	Prachin Buri	6	0	0
PC6	Hom ched chan (*Tarenna wallichii* (Hook. f.) Ridl.)	Prachin Buri	3	2	0
PC7	Sulfur Cosmos (*Cosmos sulphureus*)	Prachin Buri	3	0	0
Fruit					
CH1	Common plum (*Prunus domestica* L.)	Chiang Mai	5	0	0
CH2	Cape gooseberry (*Physalis peruviana* Linn.)	Chiang Rai	2	0	0
Total			**115**	**19**	**11**

Table 2
The distinctive carbon assimilation abilities of astaxanthin-producing isolates.

Substrates	Isolates number										
	SP3-1	SP3-2	SP3-3/1	SP3-3/4	SP3-5	SP8-7/2	SP8-8/3	SP9-10	SP9-12/2	SP9-14	SP9-15
Cycloheximide (actidione)	−	−	−	−	+	−	−	−	−	−	−
L-Arabinose	−	−	−	−	+	−	−	−	−	−	−
D-Cellobiose	+	+	+	+	+	+	−	−	−	−	−
D-Maltose	−	−	−	−	+	−	+	+	+	+	+
Potassium 2-ketogluconate	−	−	−	−	−	−	+	+	+	+	+
D-Ribose	+	+	+	−	+	+	+	+	+	+	+
L-Rhamnose	+	+	+	+	+	+	−	+	+	+	+
Palatinose	−	−	−	−	+	−	+	+	+	+	+
L-Sorbose	+	+	+	+	+	+	−	+	−	−	+
Esculin ferric citrate	+	+	+	+	+	+	+	−	−	−	+

+, positive reaction; −, negative reaction.

demonstrated positive assimilation abilities for D-galactose, D-sucrose (saccharose), D-raffinose, D-trehalose, D-mannitol, D-sorbitol, D-xylose, glycerol, L-rhamnose, potassium gluconate, and D-glucose. However, negative results were observed for *N*-acetyl-glucosamine, lactic acid, methyl-α-D-glucopyranoside, D-lactose (bovine origin), inositol, erythritol, D-melibiose, sodium glucuronate, D-melezitose, levulinic acid (levulinate), and glucosamine.

Molecular identification techniques were employed to identify the eleven astaxanthin-producing isolates, which were classified into two species: *Rhodotorula paludigena* (five isolates) and *Rhodosporidiobolus ruineniae* (six isolates), based on the amplified fragment of the D1/D2 domains of the large subunit. In the phylogenetic tree (Fig. 1), all isolates clustered with their nearest type strains. The identifications and their corresponding accession numbers are listed in Table 3. The phylogenetic tree can be seen in Fig. 1.

3.3. Genome analysis and functional annotation

Strain SP9-15, identified as *Rhodotorula paludigena* based on its phenotypic characteristics and 26S rRNA gene sequence analysis, demonstrated the ability to produce astaxanthin. Consequently, this strain was selected as the representative strain for investigating the genes and functions associated with astaxanthin production. The average nucleotide identity (ANI) values (Table 4) of the whole genomes between strain *R. paludigena* SP9-15 and other strains, including *R. paludigena* P4R5, *R. paludigena* CM33, *R. kratochvilovae* CBS 7436^T, *R. babjevae* CBS 7808^T, *R. glutinis* CBS 20^T, *R. graminis* WP1, *R. diobovata* UCD-FST 08-225, and *R. mucilaginosa* JY1105, were determined to be 99.30%, 96.40%, 80.07%, 80.05%, 79.95%, 79.79%, 79.70%, and 77.88%, respectively.

The genome of strain SP9-15 was assembled into 295 contigs, with a total length of 20,919,510 bps and a relatively high GC content of 64.21%. This assembly demonstrates notable genomic characteristics, including an N50 value of 440,396 bps, an L50 value of 18 contigs, and a maximum scaffold length of 1,411,288 bps. Interestingly, strain SP9-15 shares a similar genome size with other recognized red yeasts of the *Rhodotorula* genus, such as *R. graminis* WP1, *R. glutinis* ATCC 204091, *R. toruloides* NP11, and *Rhodotorula* sp. JG-1b, which also have genome sizes ranging from approximately 20-21 Mbp [38].

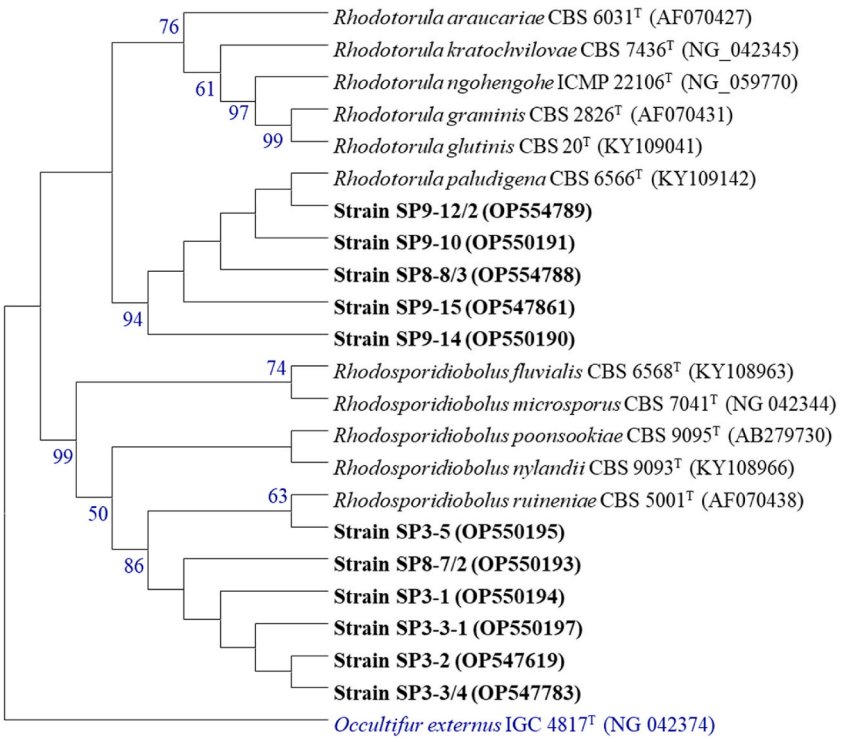

Fig. 1. The phylogenetic tree of gene sequences of 26S rRNA was generated by Maximum Likelihood method. Bootstrap values (>50%) based on 1000 replications are given at branch nodes. The GenBank accession number of each organism used is given in parentheses. Evolutionary analyses were conducted in MEGA X software.

Table 3
Strain number, nearest relative, 26S rRNA gene sequence similarity (%) of strains, and qualitative and quantitative astaxanthin production.

Isolate number	Nearest relative	Similarity (%)	Length (bps)	Accession no.	Astaxanthin production	
					Quantitative	
					Astaxanthin content (mg/g DCW)[a]	Astaxanthin yield (mg/L)[a]
SP3-1	*Rhodosporidiobolus ruineniae* CBS 5001^T	99.83	582	OP550194	0.023 ± 0.45	0.139 ± 0.003
SP3-2	(AF070438)	99.83	605	OP547619	0.039 ± 0.24	0.309 ± 0.002
SP3-3/1		99.83	595	OP550197	0.015 ± 0.87	0.104 ± 0.006
SP3-3/4		99.83	605	OP547783	0.067 ± 0.14	0.545 ± 0.001
SP3-5		100	570	OP550195	0.011 ± 0.10	0.076 ± 0.001
SP8-7/2		99.81	541	OP550193	0.022 ± 0.15	0.142 ± 0.150
SP8-8/3	*Rhodotorula paludigena* CBS 6566^T	100	581	OP554788	0.080 ± 0.21	0.701 ± 0.002
SP9-10	(NG_042,383)	100	581	OP550191	0.037 ± 0.12	0.270 ± 0.120
SP9-12/2		100	581	OP554789	0.098 ± 0.07	0.705 ± 0.070
SP9-14		100	581	OP550190	0.118 ± 0.25	1.036 ± 0.003
SP9-15		100	607	OP547861	0.147 ± 0.20	1.244 ± 0.002

[a] Mean ± standard deviation.

In Fig. 2, the circular genomics of the SP9-15 genome is illustrated, revealing the presence of 143 transfer RNAs (tRNAs) and 12 non-coding RNAs (ncRNAs) identified using the tRNAscan-SE program. Furthermore, this study adopts a comparative genomics approach to investigate genetic variations and unique characteristics that distinguish *R. paludigena* SP9-15 from closely related species. The main objective was to examine protein sequences that exhibit similarities among four yeast species: *R. paludigena* SP9-15 (7,585 proteins), *R. paludigena* P4R5 (7,703 proteins), *R. kratochvilovae* CBS 7436^T (8,257 proteins), and *R. glutinis* CBS 20^T (7,509 and 9,946 proteins), as depicted in Fig. 3. Notably, the findings of the investigation reveal that *R. paludigena* SP9-15, *R. paludigena* P4R5, *R. kratochvilovae* CBS 7436^T, and *R. glutinis* CBS 20^T have 2, 9, 173, and 368 proteins, respectively, that are unique to their respective species/strains.

Besides, the National Center for Biotechnology Information (NCBI) calculated that 6666 protein-coding genes with an average gene length of 1,524.66 bps were present in the strain SP9-15 whole-genome sequence. Furthermore, the KEGG metabolic pathway analysis

Table 4
ANI value between the draft genomes of the *R. paludigena* SP9-15; *R. paludigena* P4R5; *R. paludigena* CM33; *R. kratochvilovae* CBS 7436^{T}, *R. babjevae* CBS 7808^{T}, *R. glutinis* CBS 20^{T}, *R. graminis* WP1, *R. diobovata* UCD-FST 08-225, *R. mucilaginosa* JY1105. Genomic data: 1, *R. paludigena* SP9-15 (JAQJJA000000000); 2, *R. paludigena* P4R5 (SWEA00000000); 3, *R. paludigena* CM33 (SWEA00000000); 4, *R. kratochvilovae* CBS 7436^{T} (JACAVT000000000); 5, *R. babjevae* CBS 7808^{T} (CAKKSZ000000000); 6, *R. glutinis* CBS 20^{T} (CAKKSX000000000); 7, *R. graminis* WP1 (JTAO00000000); 8, *R. diobovata* UCD-FST 08-225 (SOZI00000000); 9, *R. mucilaginosa* JY1105 (JANBVD000000000).

Query genome	Reference genome	ANI
1	2	99.30
1	3	96.40
1	4	80.07
1	5	80.05
1	6	79.95
1	7	79.79
1	8	79.70
1	9	77.88

*Data obtained from FASTANI.

categorized 3,519 genes into five major categories: Metabolism (1,141 genes), Genetic Information Processing (748 genes), Environmental Information Processing (177 genes), Organismal Systems (86 genes), and Cellular Processes (258 genes). The genome analysis of strain SP9-15 revealed 222 genes identified by the dbCAN meta server, categorized into five classes of the Carbohydrate-Active Enzymes (CAZy) database. These classes consisted of 25 auxiliary activity (AA) genes, 18 carbohydrate esterase (CE) genes, one carbohydrate-binding module (CBM) gene, 97 glycoside hydrolase (GH) genes, and 76 glycosyltransferase (GT) genes. Notably, the detection of GH family enzymes in strain SP9-15 highlights its capability to degrade cellulose and hemicellulose, which are crucial components of plant matter. This organism can utilize lignocellulosic material for growth and survival [33].

Furthermore, the presence of glycosyltransferases (GTs) in the SP9-15 genome suggests its capacity to synthesize intricate carbohydrates, such as glycoproteins and glycolipids, which are essential for various biological functions [39]. The identification of carbohydrate-binding modules (CBMs) within the SP9-15 genome indicates its capability to recognize and bind specific carbohydrates, including those found in plant cell walls and microbial surfaces [40]. Additionally, the presence of auxiliary activities (AAs) in the SP9-15 genome, which are vital for breaking down plant biomass and recycling carbon and energy in the environment, suggests its potential to degrade lignin present in plant cell walls. This organism can utilize lignocellulose as a source for growth [41].

Collectively, these remarkable characteristics and capabilities of strain SP9-15 suggest its potential for producing astaxanthin from lignocellulose and other agricultural waste resources. By utilizing lignocellulosic materials as substrates, strain SP9-15 could contribute to the sustainable and efficient production of astaxanthin, offering a promising avenue for the agricultural industry. Table 5 presents the annotated putative genes associated with astaxanthin biosynthesis in the genome of strain SP9-15. The biosynthesis of astaxanthin involves multiple genes, including geranylgeranyl pyrophosphate synthase (*CrtE*), phytoene synthase/lycopene beta-cyclase (*CrtYB*), phytoene desaturase (*CrtI*), beta-carotene 4-ketolase/3-hydroxylase or astaxanthin synthase (*CrtS*), cytochrome

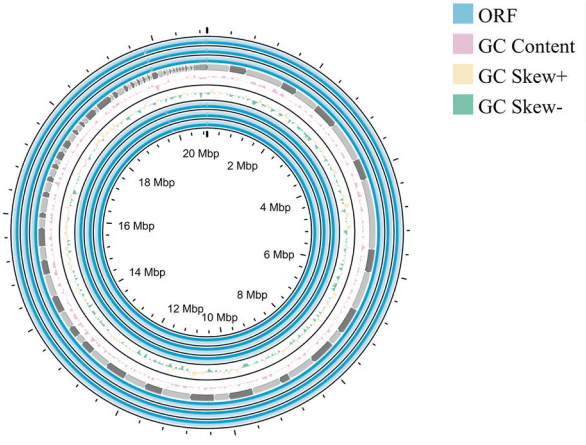

Rhodotorula paludigena SP9-15

Fig. 2. The circular genomic map of *Rhodotorula paludigena* SP9-15 displays the following information: open reading frames (ORFs) in blue, GC content in pink, GC skew (+) in yellow, and GC skew (−) in green. (For interpretation of the references to color in this figure legend, the reader is referred to the Web version of this article.)

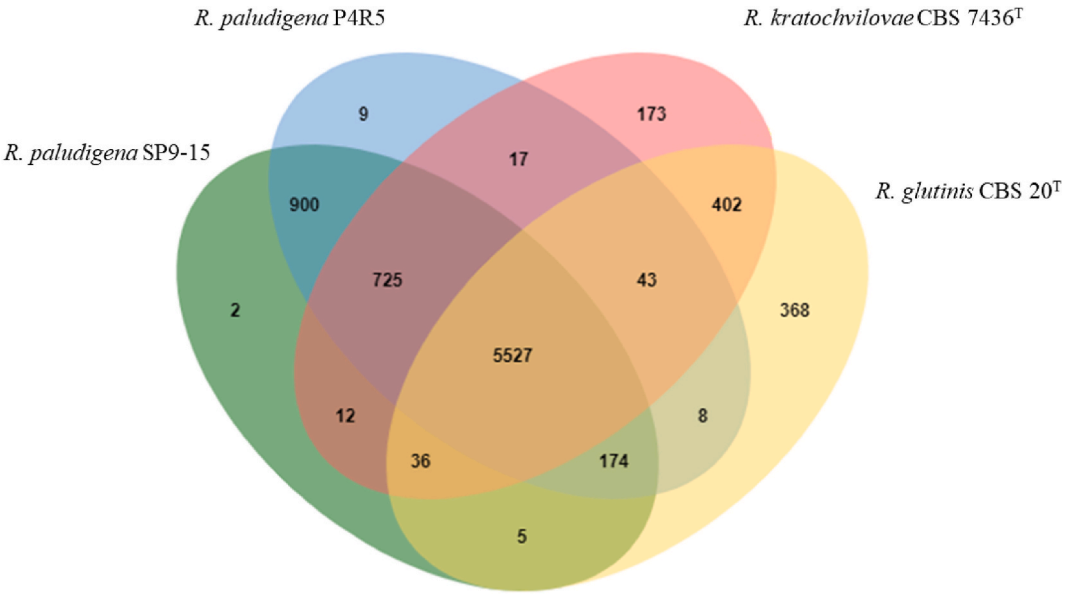

Fig. 3. Venn diagram illustrating the shared and unique protein in *Rhodotorula paludigena* SP9-15 and comparison with proteins found in *R.paludigena* P4R5, *R. kratochvilovae* CBS 7436^{T}, and *R. glutinis* CBS20^{T}, respectively.

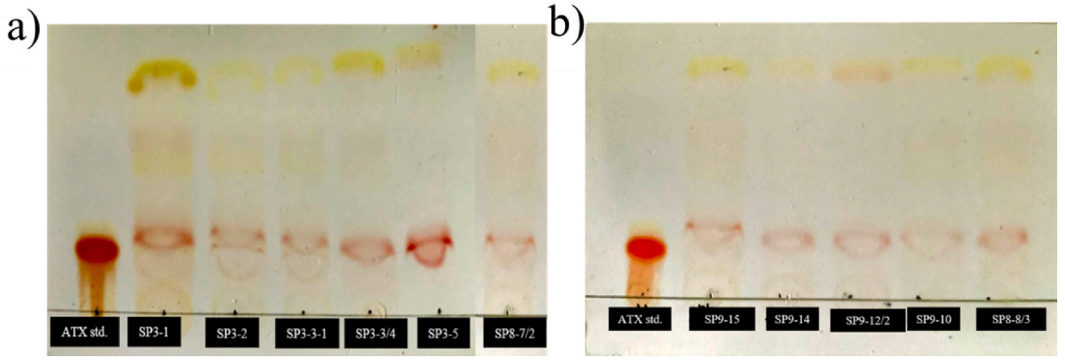

Fig. 4. Thin layer chromatography (TLC) of an acetone extract of astaxanthin-producing isolated yeasts and astaxanthin standard. The presence of astaxanthin band of several *Rhodosporidiobolus ruineniae* isolates (a), and *Rhodotorula paludigena* isolates (b).

P450 reductase (*CrtR*), beta-carotene/zeaxanthin 4-ketolase (*CrtW*), beta-carotene ketolase (*CrtO*), and beta-carotene hydroxylase (*CrtZ*), all of which were annotated in the SP9-15 genome.

In this study, potentially important enzyme genes responsible for astaxanthin production were identified and annotated in the genome of *R. paludigena* SP9-15. These enzymes, including geranylgeranyl pyrophosphate (*GGPP*), phytoene synthase (*CrtYB*), phytoene desaturase (*CrtI*), and lycopene cyclase (*CrtYB* gene), play crucial roles in the biosynthetic pathway of astaxanthin [42,43]. Additionally, the conversion of β-carotene and γ-carotene into xanthophylls is facilitated by a single enzyme called astaxanthin synthetase (*CrtS*), with the assistance of cytochrome P450 reductase (*CrtR*) [43]. Identifying and cataloging these putative genes and their predicted functions provide valuable insights into astaxanthin production in *R. paludigena* SP9-15 and exploring innovative bioprocesses to enhance its production.

3.4. Qualitative astaxanthin analysis

In Fig. 5, the qualitative analysis of astaxanthin production from all isolates is presented. The highest astaxanthin production was observed in isolate SP9-15, which was selected for confirming and optimizing astaxanthin production. The presence of astaxanthin was further confirmed by the HPLC chromatogram, where the extracted astaxanthin from isolate SP9-15 and the extracted astaxanthin with 10 ppm of the astaxanthin standard showed peaks at retention times of 2.063 and 2.083 min, respectively (Fig. 5a). Additionally, mass spectrometric analysis was employed using negative scan mode MS/MS detection. The extracted astaxanthin from isolate SP9-15 in DMSO displayed product ions (513.20, 430.75, and 348.90) that were similar to the astaxanthin standard. The astaxanthin standard

Table 5
The putative candidate astaxanthin synthesis-associated genes of the *R. paludigena* SP9-15.

Biosynthetic pathways	Putative genes	Gene product	Scaffold ID
Mevalonate	*ACAT*	Acetyl-CoA acetyltransferase (EC:2.3.1.9)	scaffold36.g5907
	HMGCS	Hydroxymethylglutaryl-CoA synthase (EC:2.3.3.10)	scaffold44.g6367
	HMGCR	Hydroxymethylglutaryl-CoA reductase (EC:1.1.1.34)	scaffold76.g7394
	PMVK	Phosphomevalonate kinase (EC:2.7.4.2)	scaffold14.g2863
	MVD	Diphosphomevalonate decarboxylase (EC:4.1.1.33)	scaffold30.g5293
Isoprene biosynthesis	*IDI*	Isopentenyl-diphosphate delta-isomerase (EC:5.3.3.2)	scaffold33.g5581
	GGPS	Geranylgeranyl diphosphate synthase (EC:2.5.1.1 2.5.1.10 2.5.1.29)	scaffold9.g1959
	FDPS	Farnesyl diphosphate synthase (EC:2.5.1.1 2.5.1.10)	scaffold12.g2635
	CrtE	Geranylgeranyl pyrophosphate synthase (EC:2.5.1.1 2.5.1.10 2.5.1.29)	scaffold9.g1959
Astaxanthin biosynthesis	*CrtYB*	Phytoene synthase/Lycopene beta-cyclase (EC:2.5.1.32 5.5.1.19)	scaffold1.g146
	CrtI	Phytoene desaturase (EC:1.3.99.30)	scaffold1.g148
Astaxanthin biosynthesis	*CrtS*	Beta-carotene 4-ketolase/3-hydroxylase (also known as astaxanthin synthase) (EC:1.14.99.63 1.14.15.24 1.14.99.-)	scaffold5.g840
	CrtR	Cytochrome P450 reductase (EC:1.14.14.1 1.6.2.4)	scaffold32.g5558
	CrtW	Beta-carotene/zeaxanthin 4-ketolase (EC: EC:1.14.99.63 1.14.99.64)	scaffold7.g1172
	CrtO	Beta-carotene ketolase (EC:1.14.99.63)	scaffold1.g148
	CrtZ	Beta-carotene hydroxylase (EC:1.14.13.-)	scaffold24.g4655

had a precursor ion (595.38) and product ions (513.20 (CE = 25.0), 430.75 (CE = 12.0), 348.90 (CE = 48.0)) (Fig. 5b).

3.5. Optimization of astaxanthin production from selected yeast strain

Among the pigmented yeast strains of the 11 isolates, *R. paludigena* SP9-15 has emerged as a promising candidate for astaxanthin production. This strain exhibited the maximum initial astaxanthin content, as determined by preliminary quantitative analysis (without shaking), with a value of 0.147 ± 0.200 mg/g DCW. Moreover, the strain SP9-15 displayed a noteworthy astaxanthin yield of 1.244 ± 0.002 mg/L in YM broth after cultivation at 25 °C for 72 h (Table 3). These findings suggest that in further studies, *R. paludigena* SP9-15 could potentially be a valuable source for optimizing astaxanthin production.

To optimize production, a study investigated the effects of key factors, such as carbon sources and concentrations, nitrogen supplementation, pH, temperature, and cultivation time, on the growth rate and astaxanthin production of *R. paludigena* SP9-15.

3.5.1. Effects of different carbon sources

The study investigated astaxanthin production by *R. paludigena* SP9-15 using four different carbon sources: glucose, maltose, fructose, and sucrose. Interestingly, the highest astaxanthin content, measured at 0.543 ± 0.024 mg/g DCW (dry cell weight), and yield, reaching 2.606 ± 0.113 mg/L, were obtained when glucose was used as the carbon source (Fig. 6a). Although sucrose supported

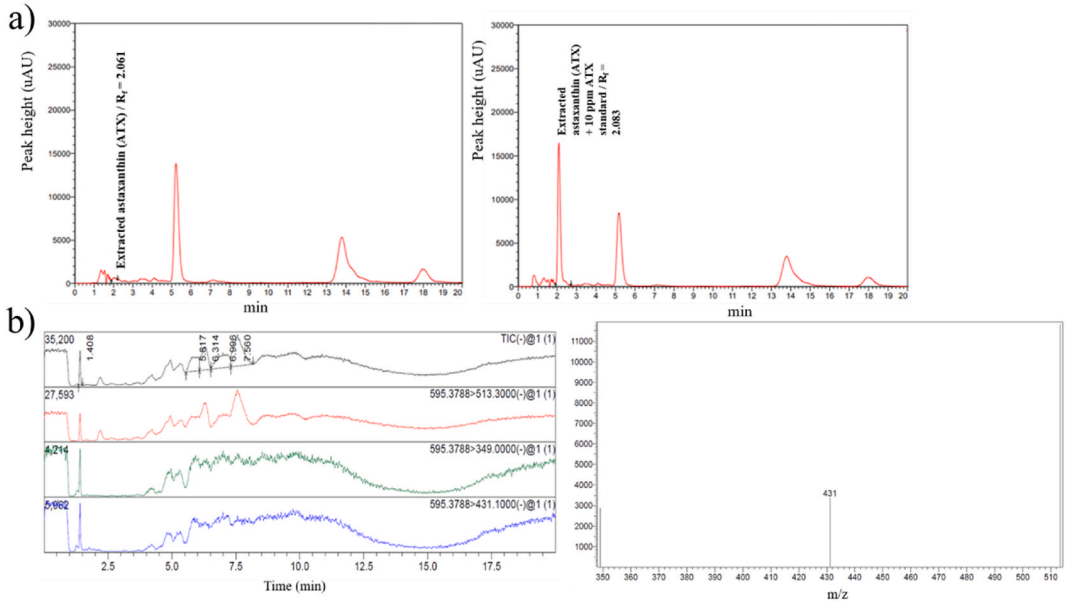

Fig. 5. The HPLC chromatogram of the extracted astaxanthin from *R. paludigena* SP9-15 in DMSO, non-spiked and spiked with a 10 ppm astaxanthin standard (a). The LC-MS chromatograms in MRM mode (negative scan) of the extracted astaxanthin from *R. paludigena* SP9-15 in DMSO (b).

cell growth up to 5.975 ± 0.001 g/L DCW, it did not yield comparable astaxanthin content, yield, and productivity. Furthermore, statistical analysis confirmed that astaxanthin production with glucose significantly differed from that with other carbon sources. Therefore, glucose was determined to be the optimal carbon source for astaxanthin production and was selected for further optimization efforts.

These findings were reinforced by the research conducted by Wu and Yu [44], which demonstrated that both glucose and sucrose effectively promoted yeast growth and astaxanthin synthesis. They observed that these carbon sources upregulate key carotenogenic genes, including *CrtI, CrtYB, CrtE*, and *CrtS* (or *ast*). In another study, *Rhodosporidium diobovatum* exhibited efficient utilization of glucose, resulting in carotenoid production of 0.324 mg/g after 144 h of fermentation [45]. Notably, glucose possesses several advantages as a carbon source for astaxanthin production. It offers a high carbon yield, exerts regulatory effects, and stands out for its availability and affordability. Glucose can be readily sourced from renewable resources like plant biomass or cornstarch, establishing it as a sustainable choice for bioprocesses [46]. Considering these compelling factors, it becomes evident that glucose emerges as the preferred carbon source for astaxanthin synthesis.

3.5.2. *Effect of glucose concentration*

As shown in Fig. 6b, increasing the glucose concentration from 10 to 40 g/L resulted in continuous improvements in astaxanthin content, yield, and productivity. At 40 g/L glucose, the highest astaxanthin content, yield, and productivity were 0.592 ± 0.015 mg/g DCW, 4.510 ± 0.111 mg/L, and 1.503 ± 0.037 mg/L/day, respectively. This represented a significant increase in astaxanthin yield, almost 5.88-fold, compared to 10 g/L glucose. Consistently, when using 10 g/L glucose as a carbon source, a biomass of 4.665 ± 0.003

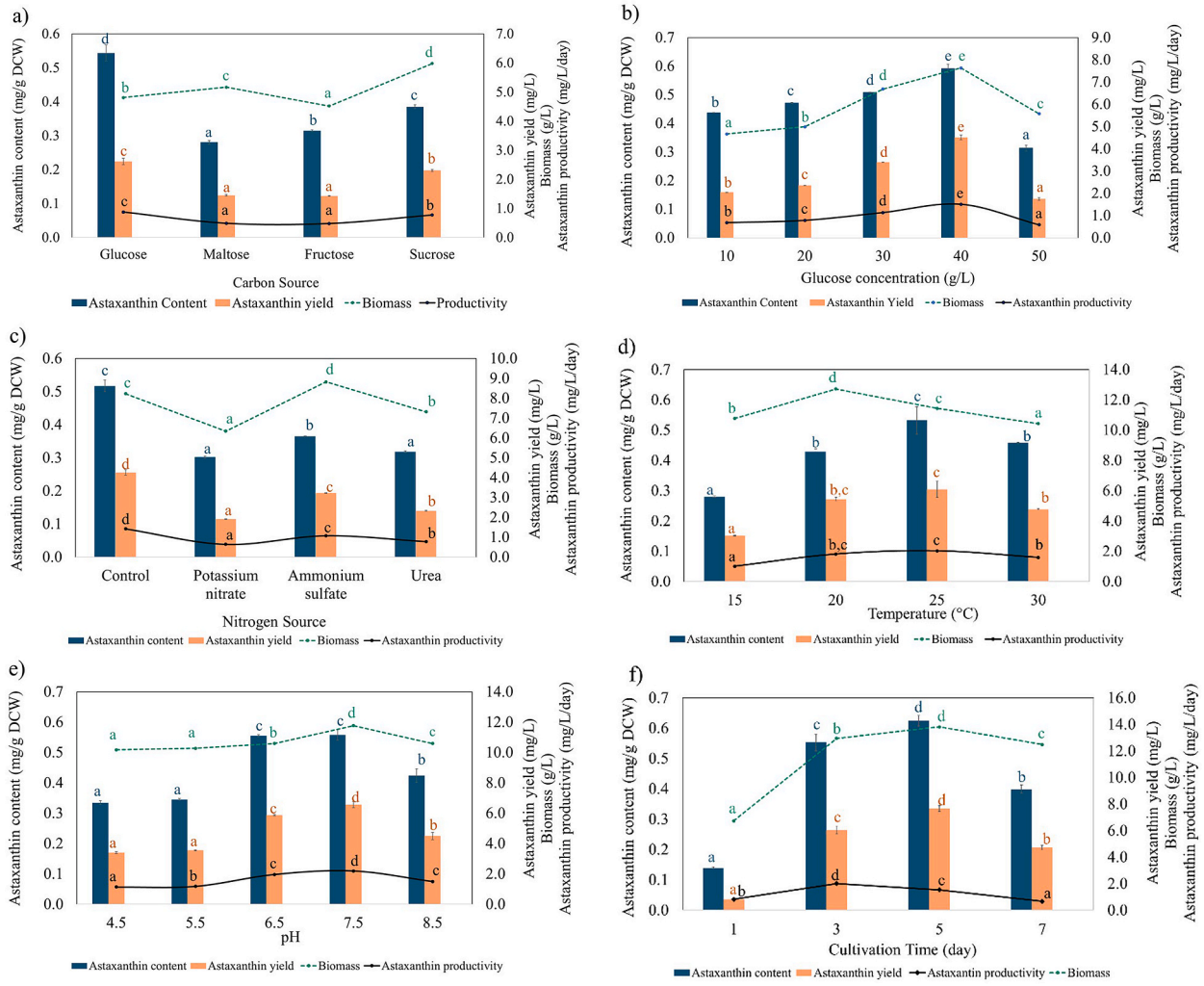

Fig. 6. Effect of carbon sources (a), glucose concentration (b), nitrogen supplementation (c), pH (d), temperature (e) and cultivation time (f) on the astaxanthin content (mg/g DCW), astaxanthin yield (mg/L), biomass (g/L), and productivity (mg/L/day) of *R. paludigena* SP9-15. The experiments were performed in triplicate, and the results were presented as the mean ± standard deviation (SD). The Tukey's test with a significance level of α 0.05 was applied, and the levels that are not linked by the same letter indicate significant differences.

g/L was obtained, similar to the previous experiment conducted under the same conditions, which yielded a biomass of 4.802 ± 0.002 g/L. However, the biomass increased significantly, reaching its highest value of 7.628 ± 0.007 g/L with 40 g/L glucose. On the other hand, increasing glucose to 50 g/L had a negative effect on astaxanthin production and biomass. This inhibition of cell growth at high glucose concentrations reduced the ability of *R. paludigena* SP9-15 to produce astaxanthin. Based on statistical analysis, a glucose concentration of 40 g/L was deemed optimal for supporting cell growth and astaxanthin production, leading to its selection for further experimentation and optimization.

The study revealed that *R. paludigena* SP9-15 possesses strong sugar fermentation capabilities, making it an attractive candidate for industrial production. Increasing the glucose concentration from 10 to 40 g/L resulted in improved cell growth and astaxanthin production. This research emphasizes the suitability of strain SP9-15 for batch cultivation. However, it was observed that raising the glucose concentration to 50 g/L had a negative impact. Consequently, to enhance astaxanthin production at higher carbon source concentrations, different cultivation modes such as batch, fed-batch, and continuous have been explored for carotenoid production in yeasts, both in laboratory and pilot-scale settings.

According to the research of Miao et al. [47], high glucose levels inhibit astaxanthin synthesis by impeding key conversion steps (the lycopene-to-β-carotene and β-carotene-to-astaxanthin) in the pathway and limiting precursor (GGPP and phytoene) transfer to carotenoids, particularly when glucose exceeds 40 g/L. Furthermore, as the glucose concentration surpasses 40 g/L, there was a rapid decline in *CrtE* expression, suggesting that glucose primarily represses astaxanthin synthesis during the production of GGPP, phytoene, and lycopene. Consequently, the β-carotene synthesis becomes the limiting factor for astaxanthin production under high glucose conditions. This phenomenon significantly hampers astaxanthin synthesis when glucose levels exceed 40 g/L, similar to previous research findings [48,49].

3.5.3. Effect of nitrogen supplementation

Besides the carbon source, nitrogen is crucial for promoting yeast growth rate and metabolism. The YM medium is rich in organic nitrogen sources and vitamins. However, inorganic nitrogen sources are more cost-effective and are typically used in lower concentrations. Tran et al. [50] studied the effect of various nitrogen sources, including organic and ammonium sulfate. Their results showed that peptone resulted in a lower biomass concentration (3.19 g/L) compared to meat extract but led to the highest astaxanthin content (0.161 mg/g) and astaxanthin concentration (0.513 mg/L) in the cultivation of *Rhodosporidium toruloides*. In contrast, another study reported that adding 0.5 g/L of urea could enhance astaxanthin production in *Rhodosporidium* sp. [9]. Furthermore, the combination of organic and inorganic nitrogen sources, such as 0.28 g/L $(NH_4)_2SO_4$, 0.49 g/L KNO_3, and 1.19 g/L beef extract, has been found to improve the production of astaxanthin from *Phaffia rhodozyma*. The optimal conditions resulted in a biomass yield of 7.71 g/L and the highest astaxanthin yield of 1.00 mg/g [51]. However, the preliminary results of this research showed that substituting organic nitrogen sources with inorganic ones led to a decrease in both biomass production and astaxanthin biosynthesis by *R. paludigena* SP9-15 (data not shown). Therefore, this study aimed to investigate the effect of supplementing the production medium with different inorganic nitrogen sources.

The impact of different inorganic nitrogen supplements on cell growth and astaxanthin production is shown in Fig. 6c. Compared to the control group (glucose concentration of 40 g/L without added inorganic nitrogen sources), the addition of potassium nitrate, ammonium sulfate, and urea did not enhance cell growth or astaxanthin production. The control medium exhibited the highest astaxanthin content, yield, and productivity at 0.517 ± 0.017 mg/g DCW, 4.253 ± 0.140 mg/L, and 1.418 ± 0.047 mg/L/day, respectively. When evaluating biomass in this experiment, the control group utilizing 40 g/L glucose as a carbon source yielded a biomass of 8.227 ± 0.012 g/L, which aligned with the results obtained in the previous experiment (7.628 ± 0.007 g/L). Compared to potassium nitrate (DCW of 6.342 ± 0.007 g/L) and urea (DCW of 7.313 ± 0.005 g/L) supplementation, the control medium showed significantly greater cell growth. Among the supplements, potassium nitrate had the lowest astaxanthin content at 0.302 ± 0.003 mg/g DCW. Ammonium sulfate promoted cell growth but did not significantly affect astaxanthin production. *R. paludigena* SP9-15 did not require inorganic nitrogen supplements for astaxanthin production. However, exploring substitutions for expensive nitrogen sources, different proportions of complex nitrogen sources, and considering the C:N ratio could potentially reduce production costs.

3.5.4. Effect of temperature

The results revealed that the highest astaxanthin content of 0.532 ± 0.045 mg/g DCW, astaxanthin yield of 6.090 ± 0.518 mg/L, and astaxanthin productivity of 2.030 ± 0.173 mg/L/day, along with a maximum biomass of 12.715 ± 0.001 g/L, were achieved at an incubation temperature of 25 °C (Fig. 6d). Nevertheless, statistical analysis revealed no significant difference in astaxanthin yield between cultures grown at 20 °C and 25 °C. Considering the energy cost and the long-term sustainability of maintaining a consistent temperature, cultivation at 25 °C (close to ambient temperature) was preferred for *R. paludigena* SP9-15 to optimize cost-effectiveness and ensure sustainable production. Another advantage of this condition was its potential applicability in scaling up to uncontrolled temperature conditions.

This result was supported by the research of Polulyakh et al. [52]. They reported that *P. rhodozyma* could synthesize a high astaxanthin content (85%) when cultivated below 30 °C. Therefore, maintaining the optimal temperature is crucial for regulating cell metabolism, including catabolic enzyme rate and protein half-life, which directly impacts metabolic processes [53].

Temperature fluctuations can influence biosynthetic pathways, including those related in carotenoid biosynthesis. The effect of temperature on carotenoid biosynthesis is species and/or strain dependent, resulting in variations in carotenoid yields [13]. Moreover, the effect of temperature on astaxanthin production may be attributed to the temperature-dependent enzyme activity in its biosynthesis [54]. For instance, Hayman et al. [55] reported that temperature regulates key enzymes, such as beta-carotene synthetase and torulene synthetase, involved in carotenoid biosynthesis.

These results emphasize the important role of cultivation temperature as a significant factor in achieving optimal astaxanthin production.

3.5.5. Effect of initial pH

Fig. 6e illustrates that the astaxanthin content did not show a significant difference between pH 6.5 and 7.5, with both pH levels resulting in similar astaxanthin contents of 0.555 ± 0.004 mg/g DCW and 0.558 ± 0.018 mg/g DCW, respectively. Moreover, when considering astaxanthin yield and productivity, the results revealed that the maximum yield of astaxanthin (6.565 ± 0.238 mg/L) and astaxanthin productivity (2.188 ± 0.069 mg/L/day) were achieved at an initial pH of 7.5. These values were significantly different from the other pH levels tested for cultivation.

Hence, based on the results obtained, an initial pH of 7.5 was determined to be the optimal pH for the production medium to achieve maximum astaxanthin production by *R. paludigena* SP9-15 in the optimized medium supplemented with 40 g/L glucose. Like Guan et al. [56], optimal medium conditions for culturing *P. rhodozyma* D3 were 32 g/L glucose, 12 g/L corn steep liquor as the nitrogen source, and an initial pH of 6.7. Under these conditions, *P. rhodozyma* D3 achieved a biomass of 6.47 g/L and an astaxanthin content of 1.41 mg/g. In contrast, another strain of red yeast, *P. rhodozyma* ATCC24202, produced a maximal astaxanthin yield of 109.23 μg AX/gWW under different conditions, specifically at 20.0 °C and pH 5.5 [4]. The influence of pH on cell growth and astaxanthin production was observed to be strain-specific, with varying effects based on the phenotypic traits of each strain. This underscores the significance of pH as a critical factor that was considered.

3.5.6. Effect of cultivation time

Extending the cultivation period from 1 to 5 days resulted in a continuous increase in cell growth and astaxanthin biosynthesis, as shown in Fig. 6f. The highest biomass of 12.282 ± 0.003 g/L was achieved after 5 days, with *R. paludigena* SP9-15 producing an astaxanthin content of 0.625 ± 0.017 mg/g DCW, astaxanthin yield of 7.670 ± 0.209 mg/L, and astaxanthin productivity of 1.534 ± 0.042 mg/L/day. After 3 days, the astaxanthin content was 0.553 ± 0.028 mg/g DCW, resulting in an astaxanthin yield of 6.044 ± 0.303 mg/L and an astaxanthin productivity of 2.015 ± 0.101 mg/L/day, with a biomass of 10.935 ± 0.001 g/L. However, prolonging the cultivation time to 7 days led to a significant reduction in astaxanthin biosynthesis and a sharp decline in biomass.

Although the maximum biomass and astaxanthin content were observed after 5 days, the astaxanthin productivity was comparatively lower at 1.534 ± 0.042 mg/L/day. In contrast, the astaxanthin productivity was higher at 2.015 ± 0.101 mg/L/day after 3 days of cultivation. Therefore, a cultivation time of 3 days may be more economically viable for astaxanthin production from *R. paludigena* SP9-15, making it suitable for further applications. Compared to the control medium (YM) at a 3-day cultivation time, the astaxanthin productivity was significantly improved by 2.32-fold from 0.869 ± 0.038 mg/L/day to 2.015 ± 0.101 mg/L/day. According to Naghavi et al. [57], the optimal cultivation period for carotenoid biosynthesis in *R. slooffiae* occurred within 72 h, indicating that carotenoid biosynthesis in yeast occurs during the late logarithmic phase and continues into the stationary phase.

4. Conclusions

In conclusion, this study successfully screened and isolated red yeast strains capable of producing astaxanthin from flowers in Thailand. Through 26S rRNA gene analysis, *Rhodotorula paludigena* and *Rhodosporidiobolus ruineniae* were identified as the astaxanthin-producing species. The selected strain for further investigation, *R. paludigena* SP9-15, exhibited high astaxanthin production, prompting its whole-genome sequencing and annotation. Genomic analysis of *R. paludigena* SP9-15 revealed several candidate genes associated with astaxanthin biosynthesis. Furthermore, the presence of carbohydrate-active enzyme genes indicated the potential utilization of agricultural waste resources for biological applications. Production experiments conducted under optimal conditions, involving 40 g/L glucose as the carbon source, pH 7.5, and cultivation at 25 °C with 200 rpm for 3 days, resulted in a significant 5-fold increase in astaxanthin yield compared to the preliminary screening. These findings provide valuable insights into the production of astaxanthin using red yeast strains from Thailand. *R. paludigena* SP9-15 demonstrates promising potential for future applications.

Author contribution statement

Sukanya Phuengjayaem: conceived and designed the experiments; performed the experiments; analyzed and interpreted the data; contributed reagents, materials, analysis tools or data; wrote the paper.

Engkarat Kingkaew: performed the experiments; analyzed and interpreted the data; wrote the paper.

Patcharaporn Hoondee: performed the experiments; analyzed and interpreted the data.

Pornchai Rojsitthisak: conceived and designed the experiments; contributed materials and analysis tools.

Boonchoo Sritularak: conceived and designed the experiments; contributed materials and analysis tools.

Worathat Thitikornpong: conceived and designed the experiments; contributed materials and analysis tools.

Natapol Pornputtapong: conceived and designed the experiments; contributed materials and analysis tools.

Somphob Thompho: performed the experiments; interpreted the data.

Somboon Tanasupawat: conceived and designed the experiments; analyzed and interpreted the data; wrote the paper.

Data availability statement

Data associated with this study has been deposited at DDBJ/EMBL/GenBank under the accession number JAQJJA000000000;

OP550194; OP547619; OP550197; OP547783; OP550195; OP550193; OP554788; OP550191; OP554789; OP550190; OP547861.

Funding statement

This research was supported by Fundamental Fund, Thailand Science Research and Innovation via Chulalongkorn University (CU_FRB65_hea (51)_060_33_04).

Declaration of competing interest

The authors declare that they have no known competing financial interests or personal relationships that could have appeared to influence the work reported in this paper

Acknowledgements

We appreciate Miss Thitikan Sappayoon and Miss Netchanok Keeratinawesuwan for supporting the experiment. In addition, we also thank the Pharmaceutical Research Instrument Center, Faculty of Pharmaceutical Sciences, Chulalongkorn University and Department of Microbiology, Faculty of Science, King Mongkut's University of Technology Thonburi for graciously providing research facilities.

Appendix A. Supplementary data

Supplementary data to this article can be found online at https://doi.org/10.1016/j.heliyon.2023.e18280.

References

[1] X. Li, X. Wang, C. Duan, S. Yi, Z. Gao, C. Xiao, S.N. Agathos, G. Wang, J. Li, Biotechnological production of astaxanthin from the microalga *Haematococcus pluvialis*, Biotechnol. Adv. 43 (2020), 107602.
[2] G. Giannaccare, M. Pellegrini, C. Senni, F. Bernabei, V. Scorcia, A.F.G. Cicero, Clinical applications of astaxanthin in the treatment of ocular diseases: emerging insights, Mar. Drugs 18 (5) (2020) 239.
[3] H. Kikukawa, C. Shimizu, Y. Hirono-Hara, K.Y. Hara, Screening of plant oils promoting growth of the red yeast *Xanthophyllomyces dendrorhous* with astaxanthin and fatty acid production, Biocatal. Agric. Biotechnol. 35 (2021), 102101.
[4] J.H. Chen, L. Liu, D. Wei, Enhanced production of astaxanthin by *Chromochloris zofingiensis* in a microplate-based culture system under high light irradiation, Bioresour. Technol. 245 (2017) 518–529.
[5] D. Dursun, A.C. Dalgıç, Optimization of astaxanthin pigment bioprocessing by four different yeast species using wheat wastes, Biocatal. Agric. Biotechnol. 7 (2016) 1–6.
[6] H. Kawahara, A. Hirai, T. Minabe, H. Obata, Stabilization of astaxanthin by a novel biosurfactant produced by *Rhodotorula mucilaginosa* KUGPP-1, Biocontrol Sci. 18 (1) (2013) 21–28.
[7] R. Rekha, K. Nimsi, K. Manjusha, T. Sirajudheen, Marine yeast *Rhodotorula paludigena* VA 242 a pigment enhancing feed additive for the ornamental fish koi carp, Aquac. Fish. (2022).
[8] E.B. Amr Abd El-Rhman, A.E.R. Amal Mohamed, E.M. Ahmed Rafik, Isolation, identification and screening of carotenoid-producing strains of *Rhodotorula glutinis*, Food Sci. Nutr. 3 (5) (2012) 627–633.
[9] Q.V. Tran, Q.C. Duong, D.K. Tran, D.N. Ngo, *Rhodosporidium* sp. growth in molasses medium and extraction of its astaxanthin by using HCl, VJSTE 55 (1A) (2017) 8–18.
[10] T. Yimyoo, W. Yongmanitchai, S. Limtong, Carotenoid production by *Rhodosporidium paludigenum* DMKU3-LPK4 using glycerol as the carbon source, Agric. Nat. Resour. 45 (1) (2011) 90–100.
[11] T.N. Tran, D.H. Ngo, N.T. Nguyen, D.N. Ngo, Draft genome sequence data of *Rhodosporidium toruloides* VN1, a strain capable of producing natural astaxanthin, Data in Brief 26 (2019), 104443.
[12] A.C. Guedes, H.M. Amaro, F.X. Malcata, Microalgae as sources of carotenoids, Mar. Drugs 9 (4) (2011) 625–644.
[13] G.I. Frengova, D.M. Beshkova, Carotenoids from *Rhodotorula* and *Phaffia*: yeasts of biotechnological importance, J. Ind. Microbiol. Biotechnol. 36 (2) (2009) 163–180.
[14] Z.T. Harith, M. de Andrade Lima, D. Charalampopoulos, A. Chatzifragkou, Optimised production and extraction of astaxanthin from the yeast *Xanthophyllomyces dendrorhous*, Microorganisms 8 (3) (2020) 430.
[15] D. Zhou, X. Yang, H. Wang, Y. Jiang, W. Jiang, W. Zhang, M. Jiang, F. Xin, Biosynthesis of astaxanthin by using industrial yeast, Biofuel. Bioprod. Biorefin. 17 (3) (2023) 602–615.
[16] U.N. Ushakumari, R. Ramanujan, Isolation of astaxanthin from marine yeast and study of its pharmacological activity, Int. Curr. Pharmaceut. J. 2 (3) (2013) 67–69.
[17] C.P. Kurtzman, J.W. Fell, T. Boekhout, The Yeasts: a Taxonomic Study, Elsevier, 2011.
[18] K. O'Donnell, L.E. Gray, Phylogenetic relationships of the soybean sudden death syndrome pathogen *Fusarium solani* f. sp. phaseoli inferred from rDNA sequence data and PCR primers for its identification, MPMI (Mol. Plant-Microbe Interact.) 8 (5) (1995) 709–716.
[19] J. Felsenstein, Evolutionary trees from gene frequencies and quantitative characters: finding maximum likelihood estimates, Evolution 35 (6) (1981) 1229–1242.
[20] S. Kumar, G. Stecher, M. Li, C. Knyaz, K. Tamura, MEGA X: molecular evolutionary genetics analysis across computing platforms, Mol. Biol. Evol. 3520 (18) (2018) 1547–1549.
[21] D.R. Zerbino, G.K. McEwen, E.H. Margulies, E. Birney, Pebble and rock band: heuristic resolution of repeats and scaffolding in the velvet short-read de novo assembler, PLoS One 4 (12) (2009), e8407.
[22] D.R. Zerbino, E. Birney, Velvet: algorithms for de novo short read assembly using de Bruijn graphs, Genome Res. 18 (5) (2008) 821–829.
[23] M. Boetzer, C.V. Henkel, H.J. Jansen, D. Butler, W. Pirovano, Scaffolding pre-assembled contigs using SSPACE, Bioinformatics 27 (4) (2011) 578–579.
[24] M. Hunt, C. Newbold, M. Berriman, T.D. Otto, A comprehensive evaluation of assembly scaffolding tools, Genome Biol. 15 (2014) 1–15.
[25] M. Boetzer, W. Pirovano, Toward almost closed genomes with GapFiller, Genome Biol. 13 (2012) 1–9.

[26] M. Stanke, O. Schöffmann, B. Morgenstern, S. Waack, Gene prediction in eukaryotes with a generalized hidden Markov model that uses hints from external sources, BMC Bioinf. 7 (1) (2006) 1–11.
[27] T.M. Lowe, S.R. Eddy, tRNAscan-SE: a program for improved detection of transfer RNA genes in genomic sequence, Nucleic Acids Res. 25 (5) (1997) 955–964.
[28] C. Jain, L.M. Rodriguez-R, A.M. Phillippy, K.T. Konstantinidis, S. Aluru, High throughput ANI analysis of 90K prokaryotic genomes reveals clear species boundaries, Nat. Commun. 9 (1) (2018) 5114.
[29] J.R. Grant, P. Stothard, The CGView Server: a comparative genomics tool for circular genomes, Nucleic Acids Res. 36 (suppl_2) (2008) W181–W184.
[30] L. Xu, Z. Dong, L. Fang, Y. Luo, Z. Wei, H. Guo, G. Zhang, Y.Q. Gu, D. Coleman-Derr, Q. Xia, OrthoVenn2: a web server for whole-genome comparison and annotation of orthologous clusters across multiple species, Nucleic Acids Res. 47 (W1) (2019) W52–W58.
[31] M. Kanehisa, Y. Sato, K. Morishima, BlastKOALA and GhostKOALA: KEGG tools for functional characterization of genome and metagenome sequences, J. Mol. Biol. 428 (4) (2016) 726–731.
[32] T. Aramaki, R. Blanc-Mathieu, H. Endo, K. Ohkubo, M. Kanehisa, S. Goto, H. Ogata, KofamKOALA: KEGG Ortholog assignment based on profile HMM and adaptive score threshold, Bioinformatics 36 (7) (2020) 2251–2252.
[33] H. Zhang, T. Yohe, L. Huang, S. Entwistle, P. Wu, Z. Yang, P.K. Busk, Y. Xu, Y. Yin, dbCAN2: a meta server for automated carbohydrate-active enzyme annotation, Nucleic Acids Res. 46 (W1) (2018) W95–W101.
[34] B.L. Cantarel, P.M. Coutinho, C. Rancurel, T. Bernard, V. Lombard, B. Henrissat, The Carbohydrate-Active EnZymes database (CAZy): an expert resource for glycogenomics, Nucleic Acids Res. 37 (suppl_1) (2009) D233–D238.
[35] R. Sharma, G. Ghoshal, Optimization of carotenoids production by *Rhodotorula mucilaginosa* (MTCC-1403) using agro-industrial waste in bioreactor: a statistical approach, Biotechnol. Rep. 25 (2020), e00407.
[36] Y. Li, F. Miao, Y. Geng, D. Lu, C. Zhang, M. Zeng, Accurate quantification of astaxanthin from *Haematococcus* crude extract spectrophotometrically, Chin. J. Oceanol. Limnol. 30 (4) (2012) 627–637.
[37] P. Casella, A. Iovine, S. Mehariya, T. Marino, D. Musmarra, A. Molino, Smart method for carotenoids characterization in *Haematococcus pluvialis* red phase and evaluation of astaxanthin thermal stability, Antioxidants 9 (5) (2020) 422.
[38] I. Fakankun, B. Fristensky, D.B. Levin, Genome sequence analysis of the oleaginous yeast, *Rhodotorula diobovata*, and comparison of the carotenogenic and oleaginous pathway genes and gene products with other oleaginous yeasts, J. Fungi 7 (4) (2021) 320.
[39] V. Lombard, H.G. Ramulu, E. Drula, P.M. Coutinho, B. Henrissat, The carbohydrate-active enzymes database (CAZy) in 2013, Nucleic Acids Res. 42 (2014) D490–D495.
[40] A.B. Boraston, D.N. Bolam, H.J. Gilbert, G.J. Davies, Carbohydrate-binding modules: fine-tuning polysaccharide recognition, Biochem. J. 382 (2004) 769–781.
[41] A. Levasseur, E. Drula, V. Lombard, P.M. Coutinho, B. Henrissat, Expansion of the enzymatic repertoire of the CAZy database to integrate auxiliary redox enzymes, Biotechnol. Biofuels 6 (2013) 1–14.
[42] C.J. Li, D. Zhao, P. Cheng, L. Zheng, G.H. Yu, Genomics and lipidomics analysis of the biotechnologically important oleaginous red yeast *Rhodotorula glutinis* ZHK provides new insights into its lipid and carotenoid metabolism, BMC Genom. 21 (1) (2020) 1–16.
[43] J.L. Barredo, C. García-Estrada, K. Kosalkova, C. Barreiro, Biosynthesis of astaxanthin as a main carotenoid in the heterobasidiomycetous yeast *Xanthophyllomyces dendrorhous*, J. Fungi 3 (3) (2017) 44.
[44] W. Wu, X. Yu, Effect of different carbon source on expression of carotenogenic genes and astaxanthin production in *Xanthophyllomyces dendrorhous*, Adv. J. Food Sci. Technol. 5 (10) (2013) 1375–1379.
[45] N. Nasirian, M. Mirzaie, N. Cicek, D.B. Levin, Lipid and carotenoid synthesis by *Rhodosporidium diobovatum*, grown on glucose versus glycerol, and its biodiesel properties, Can. J. Microbiol. 64 (4) (2018) 277–289.
[46] Z. Zhang, D. Sun, X. Mao, J. Liu, F. Chen, The crosstalk between astaxanthin, fatty acids and reactive oxygen species in heterotrophic *Chlorella zofingiensis*, Algal Res. 19 (2016) 178–183.
[47] L. Miao, S. Chi, M. Wu, Z. Liu, Y. Li, Deregulation of phytoene-β-carotene synthase results in derepression of astaxanthin synthesis at high glucose concentration in *Phaffia rhodozyma* astaxanthin-overproducing strain MK19, BMC Microbiol. 19 (2019) 1–11.
[48] M.B. Reynders, D.E. Rawlings, S.T.L. Harrison, Demonstration of the Crabtree effect in *Phaffia rhodozyma* during continuous and fed-batch cultivation, Biotechnol. Lett. 19 (1997) 549–552.
[49] G. Sandmann, Carotenoid biosynthesis in microorganisms and plants, Eur. J. Chem. 223 (1) (1994) 7–24.
[50] T.N. Tran, T. Quang-Vinh, H.T. Huynh, N.S. Hoang, H.C. Nguyen, N. Dai-Nghiep, Astaxanthin production by newly isolated *Rhodosporidium toruloides*: optimization of medium compositions by response surface methodology, Not. Bot. Horti. Agrobot. 47 (2) (2019) 320–327.
[51] H. Ni, Q.H. Chen, H. Ruan, Y.F. Yang, L.J. Li, G.B. Wu, Y. Hu, G.Q. He, Studies on optimization of nitrogen sources for astaxanthin production by *Phaffia rhodozyma*, J. Zhejiang Univ. Sci. B 8 (2007) 365–370.
[52] O.V. Polulyakh, O.I. Podoprigora, S.A. Eliseev, Y.U.V. Ershov, V.Y. Bykhovskii, A.A. Dmitrovskii, Biosynthesis of torulene and torularhodin by the yeast *Phaffia rhodozyma*, Appl. Biochem. Microbiol. (USA) (1992) 411–414.
[53] Y. Ren, J. Deng, J. Huang, Z. Wu, L. Yi, Y. Bi, F. Chen, Using green alga *Haematococcus pluvialis* for astaxanthin and lipid co-production: advances and outlook, Bioresour. Technol. 340 (2021), 125736.
[54] R. Xiao, X. Li, E. Leonard, N. Tharayil, Y. Zheng, Investigation on the effects of cultivation conditions, fed-batch operation, and enzymatic hydrolysate of corn stover on the astaxanthin production by *Thraustochytrium striatum*, Algal Res. 39 (2019), 101475.
[55] E.P. Hayman, H. Yokoyama, C.O. Chichester, K.L. Simpson, Carotenoid biosynthesis in *Rhodotorula glutinis*, J. Bacteriol. 120 (3) (1974) 1339–1343.
[56] X. Guan, J. Zhang, N. Xu, C. Cai, Y. Lu, Y. Liu, W. Dai, X. Wang, B. Nan, X. Li, Optimization of culture medium and scale-up production of astaxanthin using corn steep liquor as substrate by response surface methodology, Prep. Biochem. Biotechnol. (2022) 1–10.
[57] F.S. Naghavi, P. Hanachi, M.R. Soudi, A. Saboora, A. Ghorbani, Evaluation of the relationship between the incubation time and carotenoid production in *Rhodotorula slooffiae* and *R. mucilaginosa* isolated from leather tanning wastewater, Iran, J. Basic Med. Sci. 16 (10) (2013) 1114–1118.